The theory of free inertial currents

I. *Path and structure*

By A. R. ROBINSON and P. P. NIILER, *Pierce Hall, Harvard University*

ABSTRACT

An equilibrium theory is developed for a flow which conserves potential vorticity and consists of a stream of high relative vorticity imbedded in a geostrophic drift. Effects of bottom topography stratification and variation of Coriolis parameter are included. Transformation is made to stream axis coordinates, and a multiple expansion is made appropriate to the many scales involved. The variety of paths pertaining to flow over a uniformly sloping bottom are studied numerically. Some cross-stream profiles are obtained consistent with overall divergence. A result of importance is that a baroclinic meandering jet necessarily exchanges mass with the open ocean, i.e. a standing geostrophic wave field is a feature of the equilibrium. The broadening and narrowing of the current is obtained.

1. Introduction

Northward and eastward of Cape Hatteras the Gulf Stream flows in deep water. The mean axis of the current roughly parallels the Continental Slope and is located several hundred km to the southeast of the 500 m contour. The usual interpretation of the observational data pictures a narrow stream of high velocity which is coherent over many degrees of longitude. Although the Gulf Stream is a permanent feature of the flow in this region, the position of the stream axis wanders about. At any given time the axis presents a sinuous pattern. The amplitude of the meanders may be considerably greater than the width of the stream. A typical picture is shown in Fig. 1 (FUGLISTER & VOORHIS, 1966). The meander pattern may be almost stationary (FUGLISTER, 1963) or it may be unsteady. Transient motions have been interpreted as downstream progression of the meander pattern, and as eddy formation by the breakoff of an elongated loop (FUGLISTER & WORTHINGTON, 1951). The meandering and eddying of the stream in this region is presently the subject of considerable observational effort. The observations themselves present a complex and fascinating puzzle.

In the theory of the general circulation of the oceans, strong narrow currents play a dominant role. The interaction of the strong currents with the slower broader flow is a determinative factor in the total equilibrium of the circulation. In the simplified mathematical models which are necessarily used to study the total circulation problem such currents appear predominantly as boundary currents. However, in discussions relating the models to real oceanic flows, identification of these currents is made with the total Gulf Stream system. An understanding of free inertial currents is essential if their role is to be correctly parameterized in the study of the general circulation.

An understanding of the physics of the general circulation implies a knowledge of the overall balances of conserved quantities such as heat and vorticity. The Gulf Stream is an important mechanism for the transport and transfer of these properties. The region of meandering and eddying may be a particularly important one for communication of vorticity with the solid earth. Finally it may be remarked that an understanding of this region is of major importance in the understanding of climatological processes, on an as yet unknown scale.

The approach to the general problem adopted here is based primarily upon two previous studies, WARREN's (1963) analysis of the influence of bottom topography on the path of the free stream, and ROBINSON's (1965) general model for the three dimensional structure of inertial jets on a stratified β-plane. Here an attempt is made to penetrate the complex structure of the real geophysical situation by a consideration of many aspects of the problem.

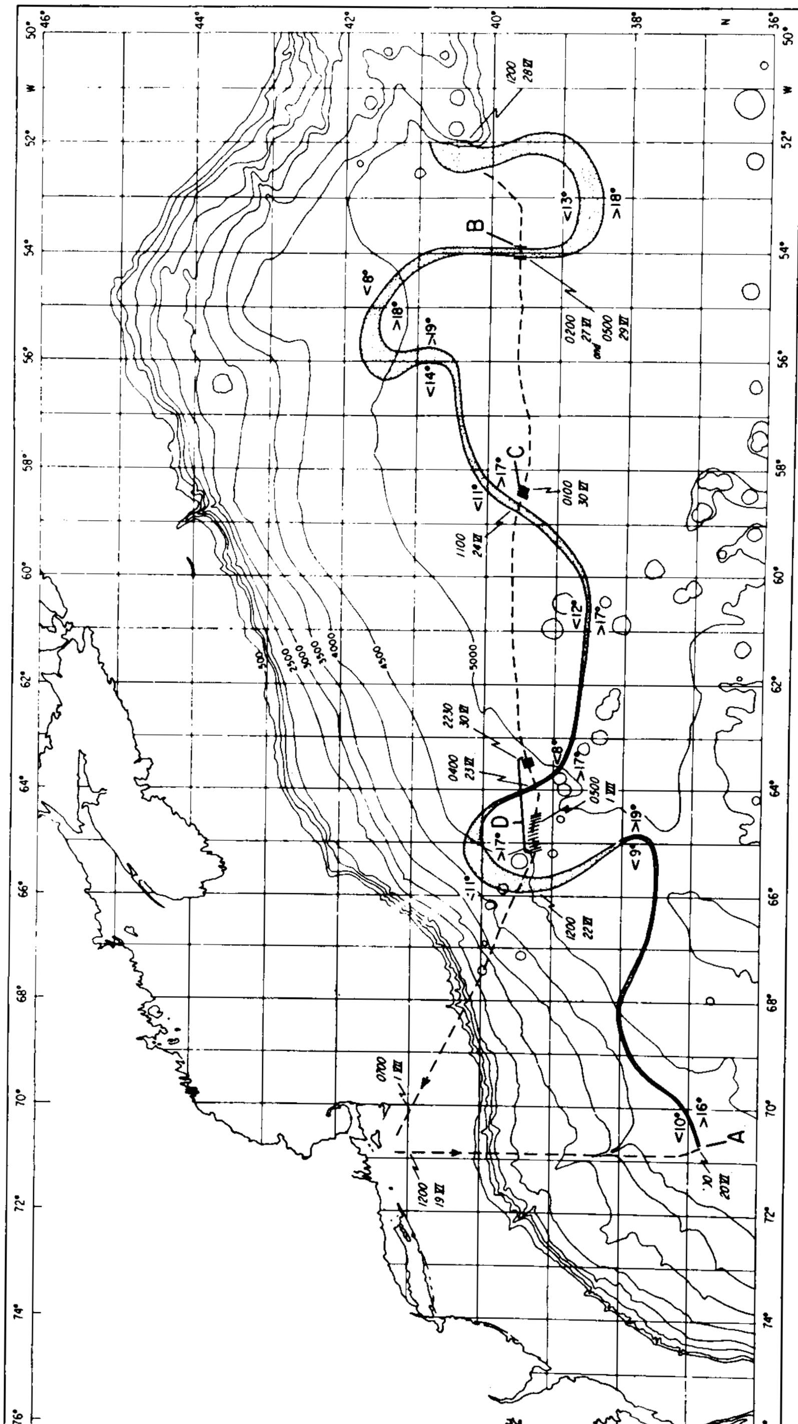

Fig. 1. The shape of the Gulf Stream as inferred from temperature measurements in late June 1964 after Fuglister and Voorhis (1966) Fig. 2.

Pieces of the problem are explored in isolation by simplified models, but often more questions are raised than answered.

This paper presents a study of free jets of simple potential vorticity distribution, which flow in equilibrium over simple bottom topography. It is the first part of a larger study. At present the equilibrium of free jets over the real topography of the North Atlantic basin is being studied by numerical analysis. The generalization of the present work to the case of time dependence is in progress.

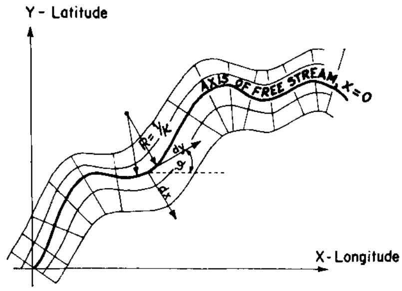

Fig. 2. The stream axis coordinates.

2. Statement of the model

2.1. Equations of the curved stream

Consider an ocean basin of semi-infinite horizontal extent and finite depth, in which the longitudinal, latitudinal, and vertical coordinates are measured respectively by $X(-\infty,\infty)$, $Y(0,\infty)$, $z(B(X, Y), H)$. Over the major part of the basin (hereafter referred to as the open ocean region) the flow is to consist of a slow and steady geostrophic motion, in which the relative vorticity is much less than the planetary vorticity due to the rotation of the earth. Let there be imbedded in the open ocean flow a limited region in which the relative vorticity is comparable to planetary vorticity. This region is identified with the inertial current. The type of free jet or current to be studied here is defined by the occurrence of the high relative vorticity region as a narrow coherent filament of high speed flow. Across the filament the pressure gradient is much larger than that characteristic of the open ocean. At each edge of the filament the pressure gradient joins smoothly to the open ocean value without the help of a solid boundary (i.e. by mass and sea-level distribution alone). It is in this sense that the current is considered to be free.

In principle the problem to be posed has the nature of a boundary value problem in (X, Y, z) space, in which a narrow area of high vorticity imposed in a boundary condition (e.g. at $(Y=0)$) would be found to result in a narrow current throughout the region of interest. But to solve directly such a complex three-dimensional boundary value problem is prohibitively difficult, even by numerical methods. In this investigation a logical approximation scheme is developed by which it is possible to treat various parts of the problem in isolation, under a set of restrictive but revealing physical assumptions. The time dependent problem, although of great interest, will not be considered. What is to be sought is an equilibrium state of the free current and the geostrophic drift.

To locate the current within the open ocean it is convenient to define an axis of the stream by some suitable means, e.g. the local velocity or vorticity maximum. To discuss succinctly the structure of the current via simplifying dynamical assumptions, it is essential to introduce a coordinate system for which the stream axis forms a coordinate line. The system to be defined is one in which the local curvature $\varkappa$ is dependent only upon the distance (y) downstream from an origin, and not upon the cross-stream distance x nor z (vid. Fig. 2). This definition is useful for the case that the stream is vertically coherent as well as narrow. The curvilinear coordinate line $x = x_0(X_0, Y_0) = 0$ forms the axis of the stream. Increments in x and y are given respectively by dx and $[1 + \varkappa(y)\, x]\, dy$, which indicates that the curvilinear coordinates are chosen in the manner that constant y are straight lines and constant x are parallel curves with the curvature $\varkappa$.

Let $\vartheta(y)$ [Fig. 2] be the angle between the coordinate line of constant x and constant Y. The transformation from x, y to X, Y coordinates has the form

$$X = \int_0^y [1+\varkappa x] \cos \vartheta dy' + x \sin \vartheta(0) \quad (2.1)$$

$$Y = \int_0^y [1+\varkappa x] \sin \vartheta dy' - x \cos \vartheta(0), \quad (2.2)$$

where $$\varkappa = \frac{d\vartheta}{dy}. \quad (2.3)$$

The physical components of velocity in the cross-stream and downstream direction are dx/dt, and $(1+\varkappa x)\ (dy/dt)$. These components are related to the velocity components along X, Y by the differential form of (2.1) and (2.2),

$$\frac{dX}{dt} = [1+\varkappa x] \cos\vartheta \frac{dy}{dt} + \sin\vartheta \frac{dx}{dt} \tag{2.4}$$

$$\frac{dY}{dt} = [1+\varkappa x] \sin\vartheta \frac{dy}{dt} - \cos\vartheta \frac{dx}{dt}. \tag{2.5}$$

The inverse transformation from X, Y to x, y coordinates exists in the region where $(1+\varkappa x) > 0$. This is the region of interest for the description of the jet properties and is the formal statement of the narrowness assumption.

The model for the dynamics of a free jet to be used here is that proposed by ROBINSON (1965) for the case that the jet is constrained to travel in a straight line ($\varkappa \equiv 0$). Identical dynamical approximations are to be made with respect to the cross-stream and down-strem directions, but in the curvilinear coordinate system defined by the jet itself. The pertinent conservation equations for momentum, mass, and density in the jet region are expressed under the Boussinesq and β-plane approximations with the neglect of all diffusive processes. Let v be the down-stream component of velocity u the cross-stream component and w the vertical component. In the usual notation, these conservation equations are written as (vid. GOLDSTEIN 1938, p. 119 for the transformation of the equations to curvilinear coordinates)

$$-\varkappa v^2 - fv + \frac{1}{\varrho_0} p_x = 0 \tag{2.6}$$

$$uv_x + vv_y + wv_z + \varkappa uv + fu + \frac{1}{\varrho_0} p_y = 0 \tag{2.7}$$

$$-gs + \frac{1}{\varrho_0} p_z = 0 \tag{2.8}$$

$$u_x + v_y + w_z = 0 \tag{2.9}$$

$$us_x + vs_y + ws_z = 0 \tag{2.10}$$

Here $s = 1 - \varrho/\varrho_0$ is the density anomaly, and the Coriolis parameter is expressed as $f = f_0 + \beta(y)$. Note that although the variation of f with latitude, Y, is linear ($f = f_0 + \beta_0 Y$), $\beta(y)$ as a function of the down-stream coordinate is a priori unspecified.

At this point reasonable boundary condition at the inlet ($y=0$), sides, top, and bottom of the jet are stated in some generality. However, an important deduction of the ensuing theory will be restrictions on the class of conditions that allow the existence of a free current in equilibrium with the surrounding open ocean. The conditions at $y=0$ are a pressure distribution $p_0(x, o, z)$ and a corresponding $s_0(x, o, z)$, $v_0(x, o, z)$. The conditions at large $|x|$, denoted by $\pm\infty$, are that the flow is independent of x and hence geostrophic,

$$v \to w \to 0, \quad fu_z^\infty + gs_y^\infty = 0. \tag{2.11}$$

The last of (2.11) represents two independent equations which hold respectively at $\pm\infty$, but the $\pm$ signs will usually be omitted in order to avoid cumbersome notation. For the application of the normal velocity condition the sea surface may be assumed undisturbed. Thus at $z=H$, and at the sea bottom, $z=B(y)$, the boundary conditions are

$$w(x, y, H) = w(x, y, B) - v(x, y, B)\, B_y = 0. \tag{2.12}$$

B is to be defined so that $B(0)=0$. In the present formulation the effects of the convergence of x-coordinate lines, cross-stream advection of u, and cross-stream variation of B and β have been neglected. These omissions are consistent with the narrowness approximation discussed above, and will be justified in subsequent sections.

If the axis of the current, and therefore the transformation of coordinates and $\varkappa(y)$ were known, equation (2.6–.12) would serve to determine the structure of the current. However, the jet axis is an unknown quantity; $\varkappa$ is a dependent variable of the problem. The curvature term is the only ageostrophic term in (2.6). The freedom of the jet together with the presence of variable depth and Coriolis parameter, obviates a completely geostrophic downstream velocity component. The curved path taken by a free current provides an ageostrophy, and the path is unique if the current is narrow and coherent (vid. Eq. 2.31 ff.). WARREN (1963) has shown how the path of a free current is determined if requisite (integral) properties of the current are known. In the present study the coupled problem of the simultaneous determination of path and properties is investigated. An approximation scheme is developed for the case that these aspects of the total flow problem are interdependent but mathematically isolatable.

2.2. Conservation of potential vorticity: The structure integral

The three-dimensional perfect fluid model posed above has been shown to have a first integral which expresses the conservation of potential vorticity (or equivalently a Bernoulli-energy integral). In addition to the boundary conditions, the free functional which appears in this integral must be specified. In reality the distribution of potential vorticity is determined by the history of the flow or by a far diffusive region. Here this physics is neglected.

A convenient device at this point is to interchange the independent roles of s and z, and to use the variable $\Pi = gsz + p$ in place of pressure. This quasi-lagrangian transformation results in the equations (vid. Robinson, 1965, for derivation),

$$-\varkappa v^2 - fv + \frac{1}{\varrho_0}\Pi_x = 0 \qquad (2.13)$$

$$uv_x + vv_y + \varkappa uv + fu + \frac{1}{\varrho_0}\Pi_y = 0 \qquad (2.14)$$

$$gz + \frac{1}{\varrho_0}\Pi_s = 0 \qquad (2.15)$$

$$(uz_s)_x + (vz_s)_y = 0 \qquad (2.16)$$

$$w = uz_x + vz_y, \qquad (2.17)$$

where the partial derivatives in x, y are taken at constant s. The system (x, y, s) independent will be called temperature space.

The form of (2.16) allows the definition of a streamlike function ψ,

$$vz_s = \psi_x, \quad uz_s = -\psi_y. \qquad (2.18)$$

The existence of ψ allows the equation for the vertical component of vorticity, formed by eliminating Π from (2.13) and (2.14), to be integrated. The result is

$$v_x + \varkappa v + f = z_s P(\psi, s). \qquad (2.19)$$

The potential vorticity $P(\psi, s)$ is in general a function of its two arguments. The specification of $P(\psi, s)$ is a constraint upon both the initial current $(y = 0)$ and the geostrophic flow with which the jet communicates at its open ocean edges. A primary effect of the s-dependence of P is uncoupled from the motion field if β is negligible. This effect is the determination of a basic stratification of the basin which remains, would the motion field vanish. The choice of s-independence implies linear stratification in this limit. In this paper, however, only the simplest case of $P = P_0$, an absolute constant, will be explored. This choice, although limiting profile shapes, can be shown to be capable of describing many features of free jets imbedded in a geostrophic drift.

It follows that in temperature space the initial profiles must be constrained to satisfy

$$-\varkappa_0 v_0^2 - f_0 v_0 + \frac{1}{\varrho_0}\Pi_{0x} = 0 \qquad (2.20)$$

$$gz_0 + \frac{1}{\varrho_0}\Pi_{0s} = 0 \qquad (2.21)$$

$$v_{0x} + \varkappa_0 v_0 + f_0 = P_0 z_{0s} \qquad (2.22)$$

$$\psi_{0x} = z_{0s} v_0. \qquad (2.23)$$

The edge boundary conditions as $x \to \pm\infty$ are governed by the equations

$$fu^\infty + \frac{1}{\varrho_0}\Pi_y^\infty = 0 \qquad (2.24)$$

$$gz^\infty + \frac{1}{\varrho_0}\Pi_s^\infty = 0 \qquad (2.25)$$

$$f = z_s^\infty P_0. \qquad (2.26)$$

Finally the vertical velocity boundary conditions become

$$w[x, y, s(H)] = 0 \qquad (2.27)$$

$$w[x, y, s(B)] = B_y v[x, y, s(B)], \qquad (2.28)$$

where the unknown surface temperatures which enter parametrically are determined from

$$z[x, y, s(H)] = H, \quad z[x, y, s(B)] = B. \qquad (2.29)$$

Here and hereafter, $s(B)$ means $s(x, y, B(y))$ and similarly for $s(H)$ etc.

CONSERVATION OF STREAMWISE AVERAGE VORTICITY: THE PATH INTEGRAL

While the potential vorticity integral determines the structure of the jet, it is the average value of the equation for the vorticity itself at each jet cross-section which determines its path. This average equation yields a first order ordinary differential equation for the curvature, and thereby implies a third order equation for the path. The curvature and direction at the origin, and the origin itself must be specified. Consider, hence, the equation which results from eliminating p from (2.6) and (2.7) and take its integral in physical space over the area of the cross-section normal to the stream,

$$\int_{x\to-\infty}^{x\to+\infty}\int_{B(y)}^{H}\left\{\frac{\partial}{\partial y}[\varkappa v^2]+v\frac{\partial\beta}{\partial y}+f\left[\frac{\partial u}{\partial x}+\frac{\partial v}{\partial y}\right]+\frac{\partial}{\partial x}[\mathbf{v}.\nabla v+\varkappa uv]\right\}dzdx=0. \quad (2.30)$$

With the help of the continuity equation and boundary conditions on v and w, this relationship simplifies to

$$\int_{x\to-\infty}^{x\to+\infty}\left\{\int_{B(y)}^{H}\left[\frac{\partial}{\partial y}(\varkappa v^2)+v\frac{\partial\beta}{\partial y}\right]dz+fv(B)\frac{\partial B}{\partial y}\right\}dx=0. \quad (2.31)$$

Note that (2.31) is an equation in y only and may be regarded as determining $\varkappa$ from the cross-sectional integral properties of the stream. If the jet were bound instead of free, the limits of the integral in (2.30) would be replaced by $x(0,\infty)$. Then the value of $(v\cdot\nabla v+\varkappa uv)_{x=0}$ would appear in (2.31). The resulting equation would merely be an identity for any solution with given $\varkappa$ (set by the boundary). The important physical difference is the ability of the solid boundary to provide any requisite pressure gradient. The free jet must seek a path consistent with the vanishing of the x-pressure gradient at both sides. This constraint is implied in (2.31).

An alternative form of the path equation is

$$\int_{x\to-\infty}^{x\to+\infty}\int_{B(y)}^{H}\frac{\partial}{\partial y}[\varkappa v^2+fv]dzdx+\int_{B(y)}^{H}f[u^{+\infty}-u^{-\infty}]dz=0. \quad (2.32)$$

In this form it may be seen simply that, at every cross-section, the rate of divergence of (average) total vorticity flux is balanced by the rate of advection of planetary vorticity from the edge of the stream. The (average) manner in which the planetary vorticity is redistributed within the stream is expressed in (2.31).

3. Exposition of path control mechanisms

3.1. DEVELOPMENT OF THE PATH INTEGRAL

Consider the path equation (2.31) in the simplest instance, i.e. that in which the bottom is flat, the Coriolis parameter is constant, and the stream is non-divergent ($B=\beta=v_y=0$). Hence, $\partial/\partial y[\varkappa\int\int_{-\infty 0}^{+\infty H}v^2\,dxdz]=0$ or $\varkappa_y=0$. The jet can maintain any circular path of constant curvature, including the limit of rectilinear flow. If there is an exchange of mass with the environment such that $v_y\neq 0$ (but with $B=\beta=0$ retained), it is the quantity $\varkappa v^2$ which is conserved along the path; the converging jet straightens and the diverging curls up.

Some mechanisms which determine the path of the stream can be simply exposed by developing (2.31) in a power series form which will be valid a short distance downstream from the origin. Let

$$v=v_0+v_1y+v_2y^2+\dots 0(y)^3 \quad (3.1)$$

and $B=B_1y+B_2y^2+\dots$, $\beta=\beta_1y+\beta_2y^2+\dots$ (3.2)

The path of the stream is described by

$$\varkappa=\varkappa_1y+\varkappa_2y^2+\dots, \quad (3.3)$$

where for the sake of the present argument $\varkappa_0=0$ has been assumed. The effect of small $\varkappa_0$ is a subject of later development in this section; if the initial curvature is large enough to control the current, only small modifications of the circular path will occur.

The zeroth and first order contributions to (2.31) appear as

$$\langle v_0^2\rangle\varkappa_1+\langle v_0\rangle\beta_1+f_0\bar{v}_0B_1=0 \quad (3.4)$$

$$2\langle v_0^2\rangle\varkappa_2+2\langle\bar{v}_0\rangle\beta_2+2f_0\bar{v}_0B_2+4\langle v_0v_1\rangle\varkappa_1-\langle v_0^2\rangle B_1\varkappa_1+\beta_1\bar{v}_1+f_0\bar{v}_{0z}B_1^2+f_0\bar{v}_1B_1+\beta_1\bar{v}_0B_1=0 \quad (3.5)$$

where for any function $\mathfrak{J}$

$$\langle\mathfrak{J}\rangle = \int_{x\to-\infty}^{x\to+\infty}\int_0^H \mathfrak{J}\,dz\,dx$$

$$\bar{\mathfrak{J}} = \int_{x\to-\infty}^{x\to+\infty} \mathfrak{J}(x,0)\,dx. \tag{3.6}$$

Let the case of bottom topographical control alone be first considered, i.e. $\beta = 0$. It may now be noted from (3.4,5) that if a straight isobath exists, it provides a possible equilibrium jet path. For the jet to maintain this path, however, it must be initially oriented correctly. In the framework of our present development the initial orientation is imposed by a choice of B_1, the rate of change of depth seen by the jet as it plunges forwards. The rectilinear path is obtained by setting $B_1 = 0$. Then by (3.4) $\varkappa_1 = 0$, whence by (3.5) $\varkappa_2 = 0$, etc. A jet following such a path may be described as a *well-adjusted well-behaved* jet. Similar paths exist over topography which contains circular isobaths, for which the well-behaved jet requires a $\varkappa_0 \neq 0$.

Consider next the case of a *well-adjusted badly-behaved* jet, i.e. the equilibrium configuration of a jet over the same rectilinear topography but in the case that the initial orientation is such that $B_1 \neq 0$. The reaction, according to (3.4), will be a curvature $\varkappa_1 = -(\bar{v}_0/\langle v_0{}^2\rangle)\, f_0\, B_1$. Thus the current may be deflected towards its original isobath (a meandering tendency) or away from it (an eddying tendency). In the northern hemisphere a meandering tendency will occur if the nearest well-behaved path has deep water on the right; an eddying tendency if on the left. It can be seen directly from (3.4) that if $B_1 = 0$, but $\beta_1 \neq 0$, similar behaviours occur.

The above considerations are valid only in the case that there exists a possible well-adjusted well-behaved path. However, in general the topography will consist of non-uniformly curved isobaths. Consider the case that the origin lies at a local point of zero curvature of an isobath. Now the best behaved jet will be one tangent to the isobath at $y = 0$; this implies $B_1 = 0$. Then (again with $\beta_1 = 0$) (3.4) yields $\varkappa_1 = 0$. Thus the stream will follow a straight line for a short distance. However the isobath will gradually curve away from this rectilinear path. Correspondingly the current leaves the isobath and sees a B_2, which in turn via (3.5) produces a $\varkappa_2$. This $\varkappa_2$ is not the curvature of the isobath itself and a meandering or eddying process is always initiated.

It is also worthwhile to point out that the meandering process does not depend solely upon the existence of a significant component of velocity at the ocean bottom (as required both by Warren's calculations and the above discussion). Again set $\beta \equiv 0$ for the sake of argument. Since the bottom velocity is zero, $\bar{v}_0 = 0$, and $\varkappa_1 = 0$ identically satisfies (3.4). Now it may be argued that, if v_1 describes a structural adjustment required to maintain equilibrium in the curved jet, $v_1 = 0$. Finally equation (3.5) yields the path tendency from

$$2\langle v_0^2\rangle \varkappa_2 + f_0 \bar{v}_{0z} B_1^2 = 0. \tag{3.7}$$

In this case the finite value of the thermal wind shear at the ocean floor controls the path, and the appearance of the B_1^2 factor favours eddying rather than meandering. The interpretation is simply that the effective bottom interaction velocity is itself proportional to the slope B_1.

Although power series development is instructive in relating path tendencies to physical processes, it is not useful for approximate calculations of actual paths. What is required is an approximation scheme which will be uniformly valid along the entire path length. Such a scheme requires expansion in a parameter rather than a coordinate. The relevant parameter is to be found by examining the assumption that the jet remain well defined and coherent in its downstream progress. The criteria that the jet remain coherent have already been mentioned in connection with the approximate dynamics expressed by equations (2.6)–(2.10). These are that the radius of curvature of the jet remains smaller than its width for all values of y, and that a significant divergence not be forced in a distance comparable to the width. It can be shown that the former is identical to the restriction that *the change of bottom depth under the jet be smaller than the mean depth of the basin.* This approximation can be introduced directly into the problem and an equation for the stream path results from (2.6)–(2.12) which is valid for all y. (See Section 5 for a formal development.)

For the path of a coherent jet with bottom velocity the approximate form of (2.31) becomes.

$$\frac{\partial}{\partial y}[\langle v^2\rangle \varkappa] + \langle v\rangle \frac{\partial \beta}{\partial y} + f_0 \bar{v} \frac{\partial B}{\partial y}. \qquad (3.8)$$

Here $v = v(x, y, z)$ is a function of the initial conditions and a forced slow divergence, i.e. v is the current which would be present in the system, were all topographical and f variations to vanish. In the case that $v(x, y, 0) = 0$, the approximate equation for the path is

$$\frac{\partial}{\partial y}[\langle v^2\rangle \varkappa] + \frac{f_0 \bar{v}_z}{2}\frac{\partial B^2}{\partial y} + \langle v\rangle \frac{\partial \beta}{\partial y} = 0. \qquad (3.9)$$

To expose the scales of the meanders as functions of the physical parameters and discern the nature of the control that topography exerts on the jet, the remaining portion of this section deals with the integration of some simple versions of the above path equations.

3.2. A uniformly sloping sea bottom

(a) The non-divergent jet with bottom velocity

For the case of a jet of constant transport, $v(x, y, x) = v_0(x, z)$, and the path equation (3.8) can be integrated once. There results

$$\langle v_0^2\rangle[\varkappa(y) - \varkappa_0] + \langle v_0\rangle \beta(y) + f_0 \bar{v}_0 B(y) = 0, \qquad (3.10)$$

where $\varkappa_0$ is the initial curvature of the stream. Let $\beta \equiv 0$ for the moment, and consider the resulting equation on a bottom which is a uniform plane of slope $\mathcal{S}$ in the Y direction,

$$\langle v_0^2\rangle \{\varkappa - \varkappa_0\} + f_0 \bar{v}_0 \mathcal{S} Y = 0. \qquad (3.11)$$

In this equation the conventions $\mathcal{S} > 0$ and $f > 0$ are adopted; the rectilinear path $Y = 0$, $x > 0$ has deep water to the right. With $\varkappa = (1 + Y'^2)^{3/2} Y''$, (3.11) determines the path as a function of latitude and longitude with the specification of $Y'(0)$ and $Y(0) = 0$. The equation can be made free of parametric coefficients if both independent and dependent variables are scaled by

$$\mathcal{L} = [\langle v_0^2\rangle / \mathcal{S} f_0 \bar{v}_0]^{1/2}. \qquad (3.12)$$

The curvature has the scale of $\mathcal{L}^{-1}$. If the width of the jet is l, this analysis is valid for $(l/\mathcal{L})^2 < 1$. Between $30 \sim 40°$N latitude, with a bottom slope of one km in a thousand, a barotropic current of 2 knots progressing through a km of water yields a meander scale (3.12) of 100 km.

The simplest example of a meandering jet occurs in the case that $|Y'(0)| < 1$ and Y' remains small everywhere. Then $\varkappa \simeq Y''$ and the scaled equation is simply $Y'' + Y = 0$. Sinusoidal meanders, $Y = Y'(0) \sin X$, result. Thus $2\pi\mathcal{L}$ is seen to be the meander wavelength and can be seen below to be the maximum wavelength for any meander over $\mathcal{S}$. To deal with more general initial conditions numerical solutions of equation (3.11) have been obtained. Fig. 3 represents the behaviour for various initial conditions when $\varkappa_0 = 0$. The effect of initial curvature on these solutions is exhibited in Fig. 4. The solutions which cross over themselves are unphysical; however, they tend to point out the conditions which lead to the formation and detaching of eddies in the stream.

Note in Fig. 3 that a jet initially directed normal to the isobaths will simply meander and progress towards positive X. In fact positive progression will occur for initial "backwards" slopes; a figure eight occurs at backward slope of ~ 1.2. Fig. 4 shows the complexity of patterns which occur even with the extremely simple topography studied here. Results not depicted on Fig. 4 were obtained for $\varkappa_0 = 10$. For this large value of initial curvature the paths were practically circular.

(b) The non-divergent jet with no bottom velocity

The pertinent equation for the path of a non-divergent jet where the bottom velocity vanishes is the integral of (3.9). Again let the bottom be of uniform slope, and $\beta \equiv 0$. Then

$$\langle v_0^2\rangle \{\varkappa - \varkappa_0\} + \frac{f_0 \bar{v}_{0z} \mathcal{S}^2 Y^2}{2} = 0. \qquad (3.13)$$

The scale and amplitude of the oscillation is now

$$\mathcal{L} = [2\langle v_0^2\rangle / \mathcal{S}^2 f_0 \bar{v}_{0z}]^{\frac{1}{3}}. \qquad (3.14)$$

A baroclinic current of linear shear with a 2 knot surface velocity in 3 km of water yields by (3.14) and $\mathcal{L} = 500$ km, with $\mathcal{S}$ and f_0 as before. If (3.13) is compared to (3.11), the effective bottom velocity is seen to be simply $v_{0z}\mathcal{S}Y$. The path equation (3.13) is also analogous to that which pertains to the flow of a current with bottom velocity over a rounded hill or valley in which $B \sim Y^2$.

The numerical solutions of the dimensionless

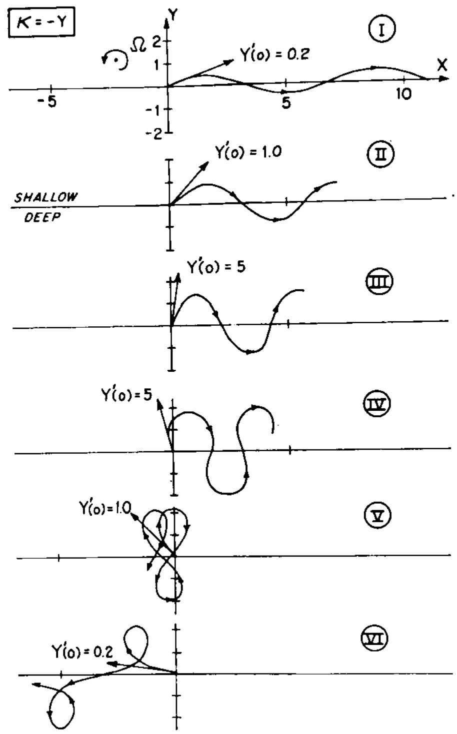

FIG. 3

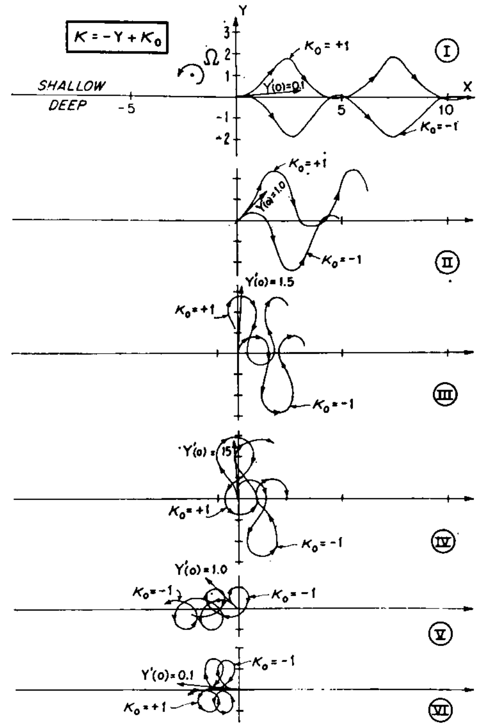

FIG. 4

Fig. 3. Stream paths over uniformly sloped bottom: bottom velocity but no initial curvature.

Fig. 4. Stream paths over uniformly sloped bottom: bottom velocity and initial curvature.

form of (3.13) are displayed in Fig. 5, and the effect of initial curvature on these solutions is found in Fig. 6. The physical or meandering solutions of (3.13) are possible only if the jet is initially ageostrophic, $\varkappa_0 \neq 0$.

(c) *The divergent jet*

Consider a jet on a uniformly sloping plane where for simplicity the down-stream component of velocity is assumed a linear function,

$$v(x, y, z) = v_0(x, z) + v_1(x, z)\,(y/\mathfrak{L}). \qquad (3.15)$$

The appropriate path equation, (3.8), is a valid approximation to the average vorticity equation when the forced divergence (v_1) is small over one meander wave-length. It is then useful to define the numbers

$$\varepsilon = z\langle v_1 v_0\rangle/\langle v_0^2\rangle, \quad r = \bar{v}_1\langle v_0^2\rangle/z\bar{v}_0\langle v_0 v_1\rangle \qquad (3.16)$$

and recall the relationships (see Fig. 2)

$$\varkappa = \frac{d\vartheta}{dy}, \quad \frac{dY}{dy} = \sin\vartheta. \qquad (3.17)$$

Let equation (3.8) be made dimensionless with respect to the $\mathfrak{L}$ of (3.12). With the help of (3.16) and (3.17) there results

$$\frac{d}{dy}[1 + \varepsilon y]\frac{d\vartheta}{dy} + [1 + r\varepsilon y]\sin\vartheta = 0, \qquad (3.18)$$

under the approximation ε very small but r of order unity. Even though ε is regarded as a small number, the effect of divergence accumulates since the path is to be predicted over many wave-lengths. This is accomplished by the rentention of terms $0(\varepsilon y)$ and the neglect of terms $0(\varepsilon)$. Equation (3.18) is to be solved for ϑ for the initial conditions at $y = 0$: $\vartheta(0) = \vartheta_0$, $d\vartheta(0)/dy = 0$.

If both $|\vartheta_0|$ and $|\vartheta(y)|$ are less than $\pi/2$, a good approximation to (3.19) is obtained by replacing $\sin\vartheta$ by ϑ. To the order of accuracy in which terms were retained in (3.18), the solution for ϑ is then obtained by the W.K.B approximation as

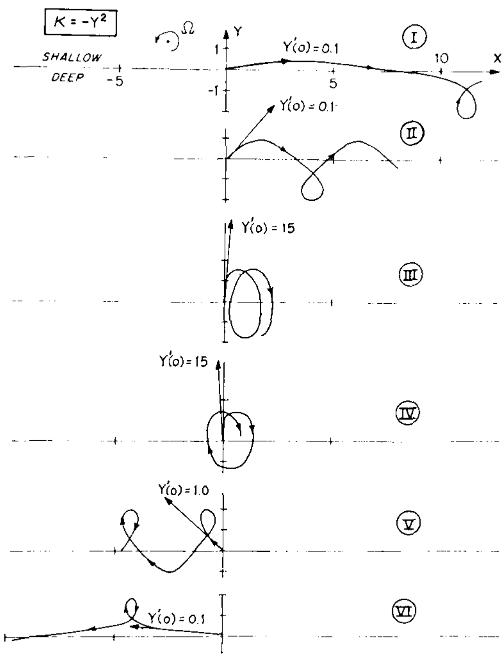

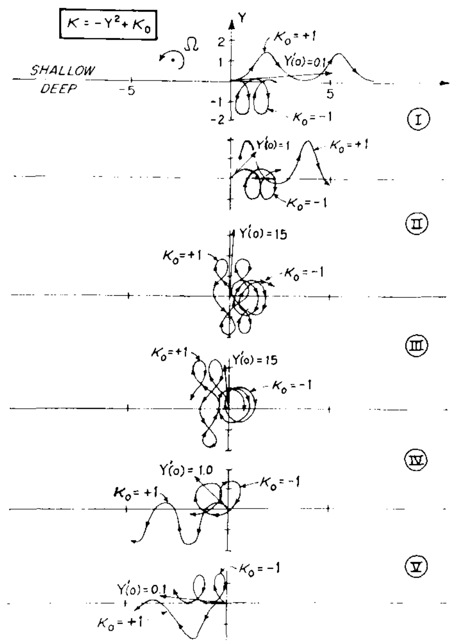

FIG. 5 FIG. 6

Fig. 5. Stream paths over uniformly sloped bottom: bottom shear but no initial curvature.

Fig. 6. Stream paths over uniformly sloped bottom: bottom shear and initial curvature.

$$\vartheta = \frac{\vartheta_0}{[1+(1+r)\varepsilon y]^{\frac{1}{4}}} \sin\left[y + \tfrac{1}{4}\varepsilon y^2 (r-1)\right]. \quad (3.19)$$

The position of the jet on X, Y grid is given by

$$X = \int_0^y \cos\vartheta(y')\,dy', \quad Y = \int_0^y \sin\vartheta(y')\,dy'. \quad (3.20)$$

If the jet is convergent ($\varepsilon > 0$), the solution indicates that oscillations of the jet tend to decrease in the down-stream direction. For a divergent jet ($\varepsilon < 0$) ϑ increases. This indicates that the solution of (3.18) would eventually form eddies by looping back on itself in an ever-increasing rate. The character of the solutions (3.20) is displayed on the schematic diagram in Fig. 7.

3.3. The case of the non-uniformly curved isobaths

The topography of a real ocean basin is at best representable only sectionally by a smooth sloping plane. Thus the solutions obtained in the above section can only apply along very short segments of a real path. These solutions can, however, be of use in the interpretation of the flow over topography in which the curvature of the isobaths is much smaller than the curvature of the meandering stream. One feature of interest can be noted upon re-examination of Figs. 3–6, viz. that in every case the line formed by connecting the points of zero curvature provides a control path for the wandering stream. That is, about equal number of equal size meanders of the stream appear on either side of this control path as the

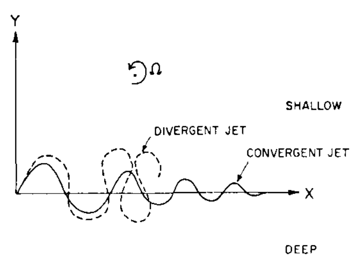

FIG. 7. Schematic representation of effect of mass transport change.

stream progresses along the uniformly sloping bottom. Now, if a stream in a real ocean basin is to continue to progress in a fashion which is a pattern of physically realizable meanders, the curvature must change sign at regular intervals. The path mapped out by simply connecting the points of zero curvature may still provide a mean control path, even for the stream in the real basin. The stream need not oscillate about a curve of $\varkappa = 0$, however if it does not, it can not remain a physically realizable stream. For to depart $\varkappa$ must be of one sign, and the stream will loop back on itself to form an eddy.

Although the definition of a curve through the zeros of $\varkappa$ as a description of a mean control path is not unique, it is a useful one and will be developed here. Other definitions were considered, e.g. the shortest curve with equal area on either side. Although such a precise definition may be ultimately useful, the excessive mathematical complexity implied proved obscurative.

For a given topography, let every $Y'(0)$ which leads to meandering over a given downstream interval be considered in turn. For each choice of such initial directions a finite number of points y_0 will occur such that $\varkappa(y_0) = 0$. The collection of such points can be seen to form, at least in certain simple instances, a dense curve. This suggests the following more general concept of a control path, viz.: the locus of all zero curvature points generated by arbitrary $Y'(0)$, which correspond to the same $v(y)$ and $\varkappa_0$. Such a locus will be called the *control curve*. It may be pointed out that for a given stream initial curvature is seen to play a more dominant role in the control of the overall path than does initial direction. This remark is particularly pertinent to the climatological mean Gulf-stream problem.

To locate control curves in some simple cases, let (3.8) be integrated by parts, whereby

$$\langle v^2 \rangle \varkappa - \langle v_0^2 \rangle \varkappa_0 + \langle v \rangle \beta + f_0 \bar{v} B - \int_0^y [\beta \langle v_y \rangle + f_0 B \bar{v}_y] dy' = 0. \tag{3.21}$$

It will be possible to treat the case of divergence only when it is a modifying effect. Thus a perturbation parameter, ε, is introduced as a measure of the change in v. Let $v = v_0(x, z) + \varepsilon v_1(x, z) y/\mathfrak{L}$, where v_0, v_1 are $0(1)$ quantities but $\varepsilon < 1$. ε is obviously related physically to the ε introduced in (3.16), but is not identical. Equation (3.21) is to be evaluated for $\varkappa(y_0) = 0$. The smallness of ε may be exploited by the neglect of the last two terms compared in each case to the related middle term. Physically this neglect is valid if the integral $\int_0^y B\, dy$ must be taken over several meanders before the change of mass becomes significant. The formal development of this approximation is accomplished in Section 5. The result is

$$- \langle v_0^2 \rangle \varkappa_0 + \langle v \rangle \beta + f_0 \bar{v} B = 0, \tag{3.22}$$

where in the coefficients $v = v_0 + \varepsilon v_1 y_0/\mathfrak{L}$. Thus the divergence effect appears parametrically and only on the last two terms; (3.22) is exact if $v_1 = 0$.

It is of interest to isolate the simple processes. For $v_1 = \beta = 0$, $B(y_0) = \varkappa_0 \langle v_0^2 \rangle / \bar{v}_0 f_0$ and the control curve is an isobath; for $\varkappa_0 = 0$, simply the initial isobath. If $\varkappa_0^{-1}$ is a radius of 500 km, and the other numbers take on values as before, a typical displacement of the control from the initial isobath is 0 (100 m). As it appears in (3.22), β is proportional to $Y(y_0)$ (recall the definition following equation (2.10)). As such its influence depends strongly on the general orientation of the stream. For $v_1 = B = 0$ the control curve is the latitude circle $\beta(y_0) = \varkappa_0 \langle v_0^2 \rangle / \langle v_0 \rangle$, the initial latitude only if $\varkappa_0 = 0$. For the initial radius of curvature of 500 km there will be displacement corresponding to only about a 1 % change in f. The β effect is of greater interest in combination with bottom topography. Then with $\varkappa_0 = 0$, the control curve is no longer tha initial siobath, but is given by $B(y_0) = -\beta(y_0) \langle v_0 \rangle / f_0 \bar{v}_0$. The maximum effect occurs when the isobaths are oriented essentially along meridians. A northward pointed stream finds a control curve falling across the isobaths into deep water. A southward control curve climbs the isobaths. A reasonable upper bound for the rate of ascent or descent is measured in hundreds of meters per thousand kilometers.

The above discussion may be modified for slow divergence by allowing the coefficients of (3.22) to vary as a function oft the particular y_0. It is seen that (for $\beta = 0$) an isobath is no longer a control curve unless $\varkappa_0 = 0$. A current which is losing mass has the displacement effect of $\varkappa_0$ enhanced over the divergenceless case.

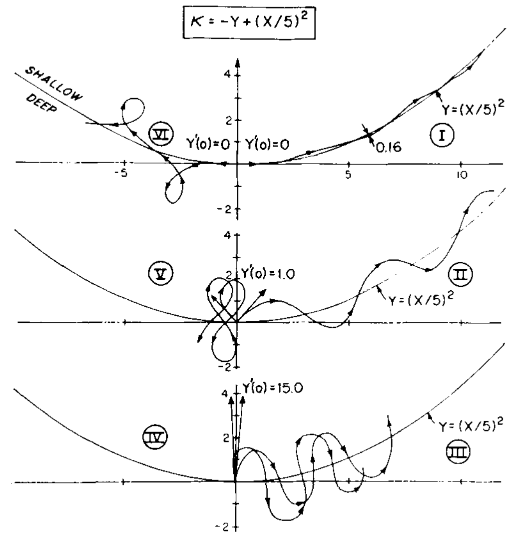

Fig. 8. Stream paths over a paraboloidal bottom.

Over the distance in which the bottom current is halved, the control curve displacement is doubled. A convergent current tends to approach the initial isobath.

A simple numerical example has been chosen to illustrate the control mechanism of the initial isobath in the case that $\beta = v_y = 0$. Actual path solutions of

$$\varkappa = -Y + (X/5)^2 \tag{3.23}$$

have been obtained and are illustrated in Figs. 8 and 9. It is seen that the solution curve oscillates about the line of zero curvature, $Y = (X/5)^2$. This example corresponds to the case where the curvature of the isobath is smaller than the curvature of the solution curve, and the solution remains oscillating about the initial isobath for a large number of meanders.

4. Influence of baroclinic meanders on the surrounding sea

In this section a final gross feature of the total free jet problem will be isolated and explored. The phenomenon to be studied is a feature of the equilibrium of the free current with the surrounding open ocean environment. Such an equilibrium will be shown to necessitate the existence of a meander scale component of geostrophic drift and is, hence, a source of intermediate scale structure to the basin. This feature of the open ocean flow will be called the *radiated wave field.* The radiated component arises from an exchange of mass of the current and the open ocean which however, does not change the average transport of the stream over many meander wave-lengths. This oscillating convergence and divergence is thus distinct from the overall change of transport discussed above. The overall divergence contributes to the determination of the jet path. In contradistinction, the radiated field (in the present model) can be calculated only after the path is known. It is a purely baroclinic phenomenon, produced by changes in the density field along the edges of the current, which are necessarily associated with the structural adjustment to the meander. Such down-stream density gradients imply thermal-wind shear and therefore a geostrophic mass exchange with the open ocean. Since the phenomenon is associated with meander produced structure, it is no longer possible to be concerned only with a stream-wise average description of the current. The example chosen to illustrate this effect is a stream of absolutely constant potential vorticity with $\beta = \varkappa_0 = 0$, and which, in the absence of topographical gradients proceeds rectilinearly with constant transport.

Consider the equations of the stream that determine the changes of structure of the jet as it moves over slowly changing bottom topography. Here let subscript $_0$ still designate the structure of the jet at $y = 0$, but symbols without subscript designate the meander induced struc-

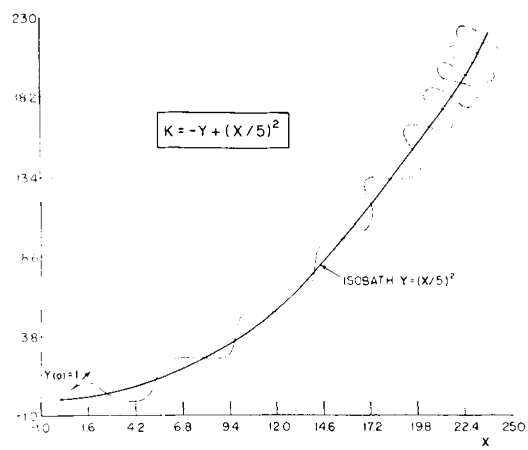

Fig. 9. Many oscillations along a parabolic control path.

tural changes. The latter are assumed to be small deviations in which the euqations are linearized. For the case of constant potential vorticity, P_0, and $\beta = 0$, these equations are obtained from (2.13)–(2.19),

$$-\varkappa v_0^2 - f_0 v + \frac{1}{\varrho_0}\Pi_x = 0 \tag{4.1}$$

$$u z_{0s} P_0 + v_0 v_y + \frac{1}{\varrho_0}\Pi_y = 0 \tag{4.2}$$

$$gz + \frac{1}{\varrho_0}\Pi_s = 0 \tag{4.3}$$

$$v_x + \varkappa v_0 = z_s P_0 \tag{4.4}$$

$$w = u z_{0x} + v_0 z_y. \tag{4.5}$$

At the sea surface and bottom the vertical velocity is given, to a consistent order of approximation, by

$$w(x, y, s_0(H)) = w(x, y, s_0(0)) - v_0(x, y, s_0(0)) B_y = 0 \tag{4.6}$$

where $s_0(H)$ and $s_0(0)$ are implicitly defined by

$$z_0(x, s_0(H)) = H, \quad z_0(x, s_0(0)) = 0. \tag{4.7}$$

At either edge of the jet the stratification must be linear; let $Sz_{0s}^{\infty} = 1$ as $x \to \pm\infty$, whence $P_0 = f_0 S$. The linear gradient must be included in the intial jet, thus $Sz_0^{\infty} = s - \mathcal{J}_0^{\pm}$ obtains on either edge of the current. Note that the sea bottom density is initially, $\mathcal{J}_0^{\pm}$, which may be different on either side. To describe the deviation field behaviour at either edge, (4.2,3,4,) may be integrated in y and s to yield the open ocean pressure field,

$$\Pi^{\infty} = \frac{\varrho_0 g}{S}\mathcal{J}(y)s - f_0\varrho_0 \int^y \mathcal{U}(y)\,dy'. \tag{4.8}$$

Thus, $Sz^{\infty} = -\mathcal{J}(y)$ (4.9)

$$u^{\infty} = -\frac{g}{Sf_0}\mathcal{J}'(y)s + \mathcal{U}(y). \tag{4.10}$$

It should be continually borne in mind that $\pm$ signs are implied throughout.

$\mathcal{J}(y)$ describes the deviation down-stream density variation and hence produces the thermal wind shear; $\mathcal{U}(y)$ is the barotropic drift component. The problem is to determine $\mathcal{J}$ and $\mathcal{U}$. To discover these functions the behaviour of the fields assymptotically *near but not at* the edge of the jet is studied. The variables are written as,

$$v_0 \sim v_0, \quad Sz_0 \sim s - \mathcal{J}_0 - \sigma_0(x, s) \tag{4.11}$$

$$s_0(H) \sim SH + \mathcal{J}_0 + \sigma_0(x, \mathcal{J}_0 + 1), \quad s_0(0) \sim +\mathcal{J}_0 + \sigma_0(x, \mathcal{J}_0) \tag{4.12}$$

$$\Pi \sim \Pi^{\infty} + \pi, \quad u \sim u^{\infty} + \mu, \quad v \sim \nu, \quad w \sim \omega, \quad z \sim z^{\infty} + \mathfrak{z}. \tag{4.13}$$

Here it is understood that ν_0, σ_0 and thus π, μ, ν, $\mathfrak{z} \to 0$ exponentially as $x \to \pm\infty$. It then follows from (4.5) that the vertical velocity field is calculated asymptotically from

$$\omega = \sigma_{0x} u^{\infty} S^{-1} + \nu_0 z_y^{\infty}. \tag{4.14}$$

Upon insertion of (4.14) into the boundary conditions (4.6, 7) and use of the thermal wind relationship which pertains asymptotically to the initial jet, there results

$$[\nu_0 - \nu_{0s}s]\mathcal{J}' + \left(\frac{Sf_0\nu_{0s}}{g}\right)\mathcal{U} = 0 \quad \text{at} \quad s = SH + \mathcal{J}_0. \tag{4.15}$$

$$(\nu_0 - \nu_{0s}s]\mathcal{J}' + \left(\frac{Sf_0\nu_{0s}}{g}\right)\mathcal{U} = -S\nu_0 B_y \quad \text{at} \quad s = \mathcal{J}_0. \tag{4.16}$$

For a simply decaying initial jet every term of (4.15, 16) contains the same exponential factor. Then it is possible to define the *constants*

$$k_0 = \left(\frac{\nu_0}{H\nu_{0z}}\right)\Big|_{z=0}, \quad k_H = \left(\frac{\nu_0}{H\nu_{0z}}\right)\Big|_{z=H}, \tag{4.17}$$

in terms of the derivatives in physical space. Now (4.17) may be substituted into (4.15, 16) which are then two simultaneous algebraic equations for $\mathcal{U}$, $\mathcal{J}'$. Upon solution the geostrophic efflux from the jet is found to be

$$u^{\infty} = \frac{gHSB_y}{f_0}\frac{k_0[k_H - 1 + z/H]}{[1 + k_0 - k_H]}, \tag{4.18}$$

and the stratification is

$$s^{\infty} = Sz + \mathcal{J}_0 + SB\frac{k_0}{[1 + k_0 - k_H]}. \tag{4.19}$$

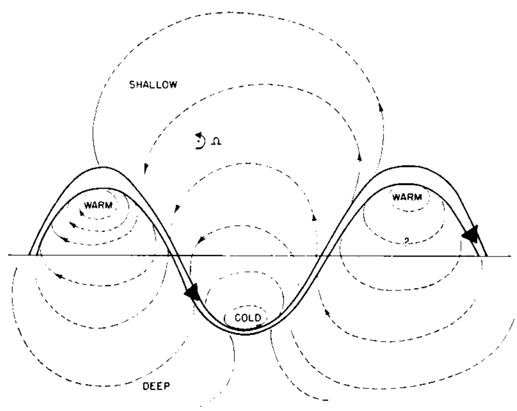

Fig. 10. Schematic description of the equilibrium of the meandering baroclinic stream and open ocean geostrophic drift.

In (4.18, 19) $\pm$signs are associated with $\mathcal{J}_0$, k_0, k_H.

The above calculation can be seen to be the first step in a consistent iterative sequence for the asymptotic behaviour of the meander generated structure. Substitution of (4.12, 13) into (4.1–5) yields after some manipulation an equation in π_0 alone. However, this equation is the asymptotic constant potential vorticity equation and is therefore merely a consistency statement. The next higher order equations determine finally the fields (4.13). Further development of the asymptotic field equations can be found in Section 7.

The radiation of a geostrophic wave by the meander as a baroclinic phenomenon is simply exposed. When the stratification vanishes, $Sk_0 \to 0$, and by (4.18)$u^\infty \to 0$. For $gHS \sim 0$ (1 cm/sec^{-2}), $B \sim 0(10^{-3})$, u^∞ is 0(10 cm/sec) times the k-factor, which is usually 0(1). It is shown below in Section 6 that asymptotically a class of constant potential vorticity jets has the property that $v_{0z} < 0$ necessarily. In this case, and if v_0 does not change sign with depth, $1 + k_0 - k_H < 0$, $k_0 < 0$, $k_H < 0$. This implies that the jet moving into shallow water is pulling water up the slope of the basin and ,moving into deep water, causes the reverse effect. The temperature of the edge of the jet increases with cyclonic meanders and decreases with anticyclonic meanders. If the jet flows in a basin that has cold water in the shallows and warm water in the deep, the cyclonic meanders will tend to produce hot pools of geostrophic water to the deep, warm side of the jet, and cold on the shallow side. The schematic structure of the meandering constant transport jet is displayed on Fig. 10. This figure is drawn for a jet of non-constant width. The width change shown has been deduced (for the constant potential vorticity jet) in Section 7.

It is of interest to compare the results of this model with observations from a real meandering ocean current. WARREN (1963) has shown that apparent agreement can be obtained between the real paths of the Gulf Stream and those calculated from the equilibrium theory path equation. The comparison of Fig. 10 and 1 is sufficiently suggestive so as to raise the question—why does a constant potential vorticity model work so well? Furthermore the observations of Swallow and Crease (CREASE, 1962) and FOFONOFF (1965) do lend themselves to an interpretation in terms of a radiated geostrophic drift. Transient velocities of the relevant scale and direction have been measured, both in the deep, as well as shallow portion of the basin adjacent to the meandering stream. Transient meandering effects are not the topic of this paper; however, even the equilibrium structure of the radiated field suggests a picture consistent with measurements in a time-scale smaller than the transient effects of the real stream. Since the stream, after leaving Cape Hatteras, moves essentially in an easterly direction, the associated radiated field would have the strongest component in the northsouth direction. The suggestion that the observation of large amplitude intermediate scale velocities in the deep water may be related to the nearby Gulf Stream was originally posed by ISELIN (1961).

5. Development of a formal approximation scheme

5.1. NON-DIMENSIONAL FORMULATION

In the previous sections approximate equations were quoted and investigated; at this point a formal statement of the assumptions and expansions will be made. The heuristic approach used above is not only revealing because of its relative simplicity, but also because it serves as a guide for the physical prejudice which is necessary to initiate a formal perturbation scheme. The essence of the scheme will be assumptions about the size of ratios of the many independent scale lengths which enter the general problem. The following scales are relevant:

l: the width of the current;
$\mathcal{L}$: the meander scale or radius of curvature;
L: the maximum relevant downstream scale (which may be the scale of the forced divergence, i.e. of the general circulation of the basin);
D: the distance between the points of maximum and minimum latitude on the path;
H: characteristic total depth (taken to be the depth at the origin);
h: characteristic bottom depth variation (or alternatively a characteristic bottom slope, S)

Non-dimensional independent coordinates are defined as

$$\xi = \frac{x}{l}, \quad \eta = \frac{y}{\mathcal{L}}, \quad \text{and} \quad \zeta = \frac{z}{H} \quad \text{or} \quad \theta = \frac{\varrho_0 s}{\Delta\varrho}, \tag{5.1}$$

where $\Delta\varrho$ is the vertical density difference.

The following considerations motivate the initial choice of scaling amplitudes of the dependent variables and internal and path dependent lengths:

(*i*) The relative vorticity v_x is to be comparable to the planetary vorticity f_0; thus v is scaled by $f_0 l$.
(*ii*) The continuity equation (2.9) is to contain no parameters; thus u, w are scaled respectively by $(f_0 l^2/\mathcal{L})$, $(f_0 lH/\mathcal{L})$.
(*iii*) The hydrostatic equation is to contain no parameter; thus Π is scaled by $(\Delta\varrho\, gH)$.
(*iv*) The ratios of horizontal pressure gradients to Coriolis accelerations are parameter independent; thus $l = (\Delta\varrho\, gH/\varrho_0 f_2^0)^{\frac{1}{2}}$, a radius of deformation.
(*v*) The control curve is not to depart very far from the initial isobath; thus depth changes are governed primarily by meandering and $h = S\mathcal{L}$.
(*vi*) The meander scale is less than the general circulation scale, and bottom velocity exists; thus the meander scale is to be given by (3.12) with $\langle v_0^2\rangle$, $\bar{v}_0$ replaced respectively by $(f_0^2\, l^3 H)$, $(f_0 l^2)$. Then $\mathcal{L} = (Hl/S)^{\frac{1}{2}}$.

Upon non-dimensionalization of the equations and boundary conditions, there appear three parameters which characterize the system, viz.

$$\varepsilon \equiv \frac{\mathcal{L}}{L}, \quad \delta \equiv \frac{h}{H} = \frac{l}{\mathcal{L}}, \quad \lambda \equiv \frac{\beta_0 D}{f_0}. \tag{5.2}$$

The solution to the problem posed is obviously dependent upon the absolute and relative sizes of δ, ε, λ. In terms of the basic geophysical quantities the first two scale ratios of (5.2) are given by

$$\varepsilon = \left[\frac{\Delta\varrho g H^3}{\varrho_0 f_0^2 S^2 L^4}\right]^{\frac{1}{4}}, \quad \delta = \frac{SL}{H}\varepsilon = \left[\frac{\Delta\varrho g S^2}{\varrho_0 H f_0^2}\right]^{\frac{1}{4}}. \tag{5.3}$$

For values typical of the North Atlantic ($\Delta\varrho/\varrho_0 = 3\times10^{-3}$, $S = 1\times10^{-3}$, $H = 4\times10^5$ cm, $L = 3\times10^8$ cm) the width of the jet $l \simeq 10^7$ cm and the meander scale $\mathcal{L} \simeq 6\times10^7$ cm, and $\varepsilon \simeq 0.2$, $\delta \simeq 0.2$. Thus both ε and δ are small and will serve as perturbation expansion parameters.

Physical interpretation of the parameters beyond that immediately provided by the definitions, will be afforded by their role in determining the amplitudes of the (non-dimensional) dependent variables. The starting point for formal expansion will be the perfect fluid equations under the Boussinesq and hydrostatic assumptions. In temperature space, the conservation of momentum, mass and density appear as

$$\delta^2\left[uu_\xi + \frac{vu_\eta}{1+\delta\varkappa\xi}\right] - \frac{\delta\varkappa v^2}{1+\delta\varkappa\xi} - fv + \Pi_\xi = 0 \tag{5.4}$$

$$uv_\xi + \frac{vv_\eta}{1+\delta\varkappa\xi} + \frac{\delta\varkappa uv}{1+\delta\varkappa\xi} + fu + \frac{1}{1+\delta\varkappa\xi}\Pi_\eta = 0 \tag{5.5}$$

$$\zeta + \Pi_\theta = 0 \tag{5.6}$$

$$\psi_\eta = -(1+\delta\varkappa\xi)\zeta_\theta u, \quad \psi_\xi = \zeta_\theta v \tag{5.7}$$

$$w = u\zeta_\xi + \frac{v\zeta_\eta}{1+\delta\varkappa\xi}. \tag{5.8}$$

The form of the Coriolis parameter is

$$f = 1 + \lambda\beta^*(\eta, \delta\xi), \tag{5.9}$$

with $\beta^* \sim 0(1)$. The arguments of β^* are written consistently with the non-dimensional form of the transformation (2.1, 2); with X, Y scaled by $\mathcal{L}$ it is only $\delta\xi$, not ξ alone, which enters. The potential vorticity integral has the form

$$-\frac{\delta^2 u_\eta}{1+\delta\varkappa\xi} + v_\xi + \frac{\delta\varkappa v}{1+\delta\varkappa\xi} + f = \zeta_\theta P(\psi, \theta). \tag{5.10}$$

The boundary conditions at the sea surface ($\zeta = 1$) and at the bottom ($\zeta = \delta b(\eta, \delta\xi)$) are

$$w[\xi,\eta,\theta(\xi,\eta,1)] = 0 \tag{5.11}$$

$$w[\xi,\eta,\theta(\xi,\eta,\delta b)] = \delta v[\xi,\eta,\theta(\xi,\eta,\delta b)]\frac{\partial b}{\partial \eta} + \delta^2 u[\xi,\eta,\theta(\xi,\eta,\delta b)]\frac{\partial b}{\partial(\delta\xi)}. \tag{5.12}$$

Note that in (5.12) the ξ-derivative has been written as $\delta(\partial/\partial(\delta\xi))$. This is because $(\partial/\partial(\delta\xi)) \sim (\partial/\partial\eta)$ necessarily when applied to b (or β^*).

To discuss the boundary condition at the open ocean edges of the current, the results of Section 4 are borne in mind. Thus, the pressure field at $\pm\infty$ is to be regarded as compounded of two parts: a forced divergence (general circulation) component (G), and a meander induced component (M). Then

$$\Pi^\infty = \Pi^G + \Pi^M, \tag{5.13}$$

and hydrostatically and geostrophically

$$\zeta^\infty = \zeta^G + \zeta^M = -[\Pi^G_\theta + \Pi^M_\theta] \tag{5.14}$$

$$u^\infty = -[\Pi^G_\eta + \Pi^M_\eta] = \varepsilon u^G + u^M. \tag{5.15}$$

The appearance of ε in (5.15) occurs because u^G is considered as an order unity function, smooth on the scale L (vid. § 5.2 below). Constant potential vorticity (now taken as $P = 1$) further requires

$$\Pi^\infty_{\theta\theta} = -f. \tag{5.16}$$

The streamwise average vorticity integral has the dimensionless form,

$$\int_{\xi\to-\infty}^{\xi\to+\infty}\int_{\delta b}^{1}\Bigg[\frac{\delta}{(1+\delta\varkappa\xi)}\frac{\partial}{\partial\eta}\left(\frac{\varkappa v^2}{(1+\delta\varkappa\xi)}\right) + \frac{\lambda}{(1+\delta\varkappa\xi)}v\frac{\partial\beta^*}{\partial\eta} + \delta\lambda u\frac{\partial\beta^*}{\partial(\delta\xi)} + \frac{\delta}{(1+\delta\varkappa\xi)}\frac{\partial}{\partial\xi}(\varkappa uv) + \frac{1}{(1+\delta\varkappa\xi)}\frac{\partial}{\partial\xi} \times ((1+\delta\varkappa\xi)\mathbf{u}\cdot\nabla v) - \frac{\delta^2}{(1+\delta\varkappa\xi)}\frac{\partial}{\partial\eta} \times (\mathbf{u}\cdot\nabla u)\Bigg]d\zeta d\xi + \int_{\xi\to-\infty}^{\xi\to+\infty} \times\left[\frac{\delta v f}{(1+\delta\varkappa\xi)}\frac{\partial b}{\partial\eta} + \delta^2 u f\frac{\partial b}{\partial(\delta\xi)}\right]d\xi = 0, \tag{5.17}$$

where $\mathbf{u}\cdot\nabla = u\dfrac{\partial}{\partial\xi} + \dfrac{v}{1+\delta\varkappa\xi}\dfrac{\partial}{\partial\eta} + w\dfrac{\partial}{\partial\zeta}$, the ξ, η derivatives are taken at constant ζ, and in the last integral u, v are evaluated at $\zeta = \delta b$. The infinite integration limits of (5.17) are to be regarded as $|\xi| > 1$ but $|\delta\xi\varkappa| < 1$. The open ocean region is to be defined by the formal limit $\delta\xi = o(1)$ as $\delta \to 0$.

5.2. The two scale expansion

At this point a formal expansion is developed under the following restrictions:

(*i*) Bottom changes are a small fraction of the total depth ($h < H$ or $\delta < 1$).

(*ii*) Significant change in transport occurs only over many meanders ($\mathfrak{L} < L$ or $\varepsilon < 1$).

(*iii*) The control curve lies at almost constant latitude.

Two mechanisms, the β-effect (λ), and topography (δ), can cause and control meandering. Three possibilities exist: one or the other process may dominate $\lambda <$ or $\gg \delta$ or the effects may be comparable $\lambda \sim \delta$. Here it is to be assumed that the β-effect may be comparable to or less than topographic. Then by the discussion preceding Equation (3.12), the latitudinal excursion will be on the order of the radius of curvature ($D = \mathfrak{L}$). Then it is convenient to replace λ by

$$\lambda^* \equiv \frac{\lambda}{\delta} = \frac{\mathfrak{L}^2\beta_0}{f_0 l} \equiv \frac{\hat\beta}{\beta^*}, \tag{5.18}$$

whence $f = 1 + \delta\hat\beta$, $\hat\beta \leq 1$. The solution to be sought in the limit defined by (*i–iii*) is the simplest in which the smallness of the parameters can be exploited while all physical processes are operative. It is also the simplest model which may be applicable to a discussion of the Gulf Stream east of Cape Hatteras.

Each dependent field, typically $\mathfrak{F}$ (ξ, η, θ; ε, δ), is to be expanded in both ε, δ, in terms of of coefficients which are smooth functions of their arguments. To insure smoothness, the correct amplitudes of the leading contribution to each field must be stated. Furthermore, in the downstream direction two scales are relevant viz. η and $\varepsilon\eta$. A representation of the solution uniformly valid over many meanders can be obtained by treating each of these quantities as distinct independent variables (Lighthill, 1949). The required form

$$\mathfrak{F} = \mathfrak{F}_0(\xi, \varepsilon\eta, \theta) + \delta\mathfrak{F}_1(\xi, \eta, \varepsilon\eta, \theta) + \ldots, \tag{5.19}$$

is to be substituted into the equation. The terms independent of δ describe the divergent jet in the absence of topography, and the $0(\delta)$ terms govern the path and describe the meander induced deviations to a first approximation. Moreover, in the $0(\delta)$-equations, terms $0(\varepsilon)$ are to be ignored, while terms $0(\varepsilon\eta)$ are to be retained. This is because in following the stream over many meanders, the interval in η is $(0, \varepsilon^{-1})$. It is anticipated that the η-dependence of $\mathfrak{J}$ is oscillatory but the $\varepsilon\eta$-dependence, monotonic. The physical nature of the approximation is simply that the local average properties of the stream govern the path over each meander, although the gradients of these properties are negligible.

The monotonic forced divergence on the general circulation scale is considered to be approximately independent of the detailed path. Thus it is specified à priori as uniform in $(\varepsilon\eta)$, and ROBINSON's (1965) downstream expansion is employed to simplify the calculation of the $\mathfrak{J}_0$ state. Typically,

$$\mathfrak{J}_0 = \mathfrak{J}_{00}(\xi,\theta) + \varepsilon\eta\mathfrak{J}_{01}(\xi,\theta), \tag{5.20}$$

where $\mathfrak{J}_{00}$ will be referred to as the initial state and $\mathfrak{J}_{01}$ as the divergent state. Finally it can be noted from an examination of the equations of § 5.1, especially (5.12, 15) that the leading contributions to the cross-stream and vertical velocities are not $0(1)$. Each has a leading general circulation contribution $0(\varepsilon)$ and meander induced contribution $0(\delta)$.

Thus the full expansion of the dependent variables has the form

$$\Pi = \Pi_{00} + \varepsilon\eta\pi_{01} + \delta\Pi_1 + \ldots \tag{5.21}$$

$$u = \varepsilon u_{01} + \delta u_1 + \ldots \tag{5.22}$$

$$v = v_{00} + \varepsilon\eta v_{01} + \delta v_1 + \ldots \tag{5.23}$$

$$w = \varepsilon w_{01} + \delta w_1 \ldots \tag{5.23}$$

$$\zeta = \zeta_{00} + \varepsilon\eta\zeta_{01} + \delta\zeta_1 + \ldots \tag{5.25}$$

$$\varkappa = \varkappa_0 + \delta\varkappa_1 + \ldots \tag{5.26}$$

where the independent variables which occur in the arguments of the expansion coefficients are demonstrated in (5.19, 20), except that $\varkappa_0 = \varkappa_0(\eta)$ only. Equations (5.21–6) are substituted into the equations of § 5.1, which are then ordered as described above. The results quoted below are for the special case of constant potential vorticity, $P = 1$.

The initial state is any solution of

$$-v_{00} + \Pi_{00\xi} = 0 \tag{5.4a}$$

$$\zeta_{00} + \Pi_{00\theta} = 0 \tag{5.6a}$$

$$v_{00\xi} + 1 = \zeta_{00\theta}. \tag{5.10a}$$

The divergent state is calculated from

$$-v_{01} + \Pi_{01\xi} = 0 \tag{5.4b}$$

$$u_{01}(v_{00\xi} + 1) + v_{00}\, v_{01} + \Pi_{01} = 0 \tag{5.5b}$$

$$\zeta_{01} + \Pi_{01\theta} = 0 \tag{5.6b}$$

$$w_{01} = u_{01}\,\zeta_{00\xi} + v_{00}\,\zeta_1 \tag{5.8b}$$

$$v_{01\xi} = \zeta_{01\theta}. \tag{5.10b}$$

The boundary conditions for the divergent state at the sea surface and bottom are

$$w_{01}[\xi, \theta_{00}(1)] = w_{01}[\xi, \theta_{00}(0)] = 0, \tag{5.11b}$$

where $\zeta_{00}(\xi, \theta_{00}(1)) = 1, \quad \zeta_{00}(\xi, \theta_{00}(0)) = 0.$ (5.27)

The surrounding geostrophic drift is specified by

$$u^G_{01} + \Pi^G_{01} = 0 \tag{5.14b}$$

$$\zeta^G_{01} + \Pi^G_{01\theta} = 0, \tag{5.15b}$$

where, as usual, two sets of equations ($\pm\infty$) are implied.

The path to zero order is calculated from

$$\frac{\partial}{\partial\eta}[\langle v_0^2\rangle\varkappa_0] + \langle v_0\rangle\frac{\partial\hat{\beta}}{\partial\eta} + \bar{v}_0\frac{\partial b}{\partial\eta} = 0, \tag{5.17c}$$

with $\hat{\beta}$ and b evaluated at $\xi = 0$ here and below. The equilibrium state forced by the meandering stream has the equations

$$\varkappa_0 v_0^2 + \hat{\beta} v_0 + v_1 - \Pi_{1\xi} = 0 \tag{5.4c}$$

$$u(1 + v_{0\xi}) + v_0\, v_{1\eta} + \Pi_{1\eta} = 0 \tag{5.5c}$$

$$\zeta_1 + \Pi_{1\theta} = 0 \tag{5.6c}$$

$$w_1 = u_1\,\zeta_{0\xi} + v_0\,\zeta_{1\eta} \tag{5.8c}$$

$$v_{1\xi} + \varkappa_0\, v_0 + \hat{\beta} = \zeta_{1\theta}. \tag{5.10c}$$

The boundary conditions for the meandering jet are,

$$w_1(\xi, \eta, \theta_0(1)) = 0 \qquad (5.11\,c)$$

$$w_1(\xi, \eta, \theta_0(0)) - b_\eta(\eta, 0)\, v_0(\xi, \eta, \theta_0(0)) = 0, \quad (5.12\,c)$$

where $\zeta_0(\xi, \theta_0(1)) = 1, \quad \zeta_0(\xi, \theta_0(0)) = 0. \qquad (5.28)$

The seaward geostrophic relations ($\pm\infty$) are

$$u_1^M + \Pi_{1\eta}^M = 0 \qquad (5.14\,c)$$

$$\zeta_1^M + \Pi_{1\theta}^M = 0 \qquad (5.15\,c)$$

$$\Pi_{1\theta\theta}^M = -\hat{\beta}. \qquad (5.16\,c)$$

The approximate equations reveal simply the physical nature of the perturbation scheme. The initial state is specified at $\eta = 0$ by obtaining a solution of equations (*a*). Then the slow change of transport and consequent adjustment necessary to maintain the potential vorticity distribution is calculated from equations (*b*). Since the average stream is known approximately, the curvature is given directly from (5.17c). Then the path may be computed and the meander induced structural changes obtained from equations (*c*). The formal derivation of the equations with no bottom velocity in the initial state, e.g. (3.9), is entirely analogous to the case treated here. $0(\delta)$ terms vanish but not those $0(\delta^2)$.

The small δ, ε limit investigated here may have an importance beyond merely that of accessibility of solution in a geophysically interesting parameter range. The double interpretation of δ (equation (5.2)) indicates that this may be the only range in which a free jet may remain coherent over many meanders.

6. Structure of some currents of constant potential vorticity

The structure of the meandering jet as well as the structure of the adjoining open ocean depends upon the initial state at $\eta = 0$. An investigation of general conditions presents a formidable problem; here only the simplest case of absolutely constant potential vorticity is explored. This choice hopefully will allow physical features inherent in more general jets to be exposed. This argument is a priori strengthened if P is a smooth function and does not vanish for zero arguments. A posteriori justification lies in the features of real currents which occur even in this case. The underlying cause of such agreement itself presents a fascinating physical puzzle.

The pertinent equations (5.4a, 6a, 10a) can be combined into a single equation for the dynamic pressure Π_{00}

$$\Pi_{\xi\xi} + \Pi_{\theta\theta} = -1, \qquad (6.1)$$

with the suppression of subscripts here and for the remaining portion of this section. On the open ocean edges the solution must become ξ-independent. Thus the boundary conditions are

$$\Pi(\pm\infty, \theta) \equiv \Pi_{00}^G \Pi_{00}^G = -\frac{\theta^2}{2} + \mathcal{J}^\pm \theta + \mathcal{C}^\pm. \quad (6.2)$$

For the moment, the boundary conditions on surfaces $\zeta = 0$, 1 are left arbitrary.

The solution for Π is required to have a jet-like character and only the case of a continuous velocity field will be investigated. On physical grounds regions of $(\zeta_\theta) = (\theta_\zeta)^{-1} < 0$ are to be excluded from the jet. From (5.10a) this can be seen to imply a restriction on the magnitude of cyclonic relative vorticity which is allowed within the jet region. For a current which decays simply towards the open ocean, $v_\xi = \Pi_{\xi\xi} < 0$ for $\xi > 0$. This in turn implies restrictions on $\mathcal{J}^\pm$, $\mathcal{C}^\pm$ which must be chosen in the manner that the relative vorticity of the jet is always smaller than the planetary vorticity (i.e. as the local Rossby number of this jet passes through unity the stratification formally flips from positive to negative infinity).

In physical space (6.1) corresponds to a nonlinear partial differential equation for Π, and in general only numerical solutions could be obtained to this problem for a given set of boundary conditions on $\zeta = 0$, 1. Here a simpler point of view is adopted. The problem is solved only for a class of boundary conditions that are capable of description by a particular, simple representation in θ-space. Some insight into the role of the boundary conditions is afforded by the heat conduction analogue which obtains by interpreting Π as a temperature. Then the boundary conditions on $\zeta = 0$, 1 provide a surface heat flux to balance the internal source of (6.1).

The class of solutions chosen decays exponentially in both directions about a vertical axis at $\xi = 0$. Different representations ($\pm$) of the solution to (6.1) are introduced for $\xi \gtrless 0$ and joined at the origin. Let

$$\Pi^{+} = -\frac{\theta^2}{2} + \sum_{0}^{\infty} A_n^{+} \cos(\alpha_n \theta^*) \exp(-\alpha_n \xi), \quad (6.3)$$

where $\mathcal{J}^{+} = \mathcal{C}^{+} = 0$ fixes the reference level of temperature and dynamic pressure at $\xi \to +\infty$. For $\xi < 0$, the representation is

$$\Pi^{-} = -\frac{\theta^2}{2} + \mathcal{J}^{-}\theta + \mathcal{C}^{-} + \sum_{0}^{\infty} A_n^{-} \times \cos(\alpha_n \theta^*) \exp(\alpha_n \xi). \quad (6.4)$$

In the above, $\alpha_n = [(n+\frac{1}{2})\pi]/[\theta_2 + \theta_1]$, $\theta^* = \theta + \theta_1$. θ_2, θ_1 are constant which together with $\mathcal{J}^{-}$, $\mathcal{C}^{-}$ provide the generality available in these solutions. (The superscripts on $\mathcal{J}$, $\mathcal{C}$ may now be dropped.)

The continuity of Π, Π_ξ at $\xi = 0$, requires that

$$\mathcal{J}\theta + \mathcal{C} + \sum A_n^{-} \cos(\alpha_n \theta^*) - \sum A_n^{+} \cos(\alpha_n \theta^*) = 0, \quad (6.5)$$

and

$$A_n^{-} + A_n^{+} = 0. \quad (6.6)$$

The coefficients $A_n^{\pm}$ are obtained by expanding $\mathcal{J}\theta + \mathcal{C}$ in a fourier series on the interval $-\theta_1 \leqslant \theta \leqslant \theta_1 + \theta_2$.

A simple calculation results in

$$A_n^{+} = -A_n^{-} = (\theta_1 + \theta_2)\left\{\frac{(-1)^n}{\alpha_n}(\theta_2 \mathcal{J} + \mathcal{C}) - \frac{1}{\alpha_n^2}\mathcal{J}\right\}. \quad (6.7)$$

The explicit series solutions are

$$\zeta^{+} - \theta = -\sum_{0}^{\infty} A_n^{+} \alpha_n \sin \alpha_n \theta^* \exp(-\alpha_n \xi) \quad (6.8)$$

$$\zeta^{-} - \theta = -\mathcal{J} + \sum_{0}^{\infty} A_n^{+} \alpha_n \sin \alpha_n \theta^* \exp(\alpha_n \xi) \quad (6.9)$$

$$v^{\pm} = -\sum_{0}^{\infty} A_n^{+} \alpha_n \cos \alpha_n \theta^* \exp(\pm \alpha_n \xi). \quad (6.10)$$

The series may be summed at $\xi = 0$; there results

$$\zeta(0, \theta) - \theta = -(\mathcal{J}/2) \quad (6.11)$$

$$v(0,\theta) = -\frac{(\theta_2 \mathcal{J} + \mathcal{C})}{2(\theta_1 + \theta_2)}\left[\cos\left(\frac{\pi\theta^*}{2}\right)\right]^{-1} - \mathcal{J}\frac{ln}{\pi}\left[\cos\left(\frac{\pi\theta^*}{4}\right)\right]. \quad (6.12)$$

For the class of solutions obtained here the water at $\xi \to -\infty$ is colder at every level by an amount $-\mathcal{J}$ than the water at $\xi \to +\infty$. The total difference of dynamic pressure across the jet is $\mathcal{C} + \mathcal{J}[\zeta - \mathcal{J}]$. The axis of the jet at ($\xi = 0$) has at every level the mean temperature between the two sides. The half-width of the jet compared to the radius of deformation (l) is $(\alpha_0)^{-1}$; θ_1 sets the variation of bottom temperature. If $\theta_1 = 0$, the line $\theta = 0$ corresponds to $\zeta = 0$.

A more detailed description is dependent upon the values of the arbitrary constants. These constants have been tacitly assumed 0(1) but otherwise unrestricted. Consideration of the solution, however, indicates that not all 0(1) values lead to physically acceptable results. To avoid the singularities in (6.12) it is required that $\theta_1 > -(\mathcal{J}/2)$, $\theta_2 > -(1 + \mathcal{J}/2)$. The general limiting relationship between $\mathcal{J}$, $\mathcal{C}$, θ_1, θ_2 such that $v_\xi > -1(\zeta\theta > 0)$ has not been found.

Numerical inversions of the solutions from temperature space to physical space have been made for two particular sets of values of the parameters. Fig. 11 represents the inversion of the solution for the density field when $\theta_1 = \mathcal{J} = 0$, $\mathcal{C} = -1$, $(2\theta_2/\pi) = 1$. It is seen that a limit line $(\partial\zeta/\partial\theta = 0)$ intrudes into the region $(0 \leqslant \zeta \leqslant 1)$, and single valued solutions cannot be found for such scaling of the problem for all ζ. Figure 12 is a similar picture for $\mathcal{J} = -0.4$, $[2(\theta_1 + \theta_2)/\pi] = 1$, $(\mathcal{C} + \theta_2\mathcal{J}) = -1$, $\theta_1 = 0.4$. In the latter case a limit line intrudes even further into the region.

In figures (11, 12) the regions of the solutions regarded as examples of possible constant potential vorticity jets lie below the furthermost point of intrusion of the limit line. This region could be scaled to unity in a new ζ variable, but this has not been done. To do so meaningfully an extensive calculation of intrusion depth as a function of the arameters would be necessary. It also might be remarked that two layer models of boundary inertial currents become invalid (singular) precisely in the limit where the relative vorticity becomes equal to plane-

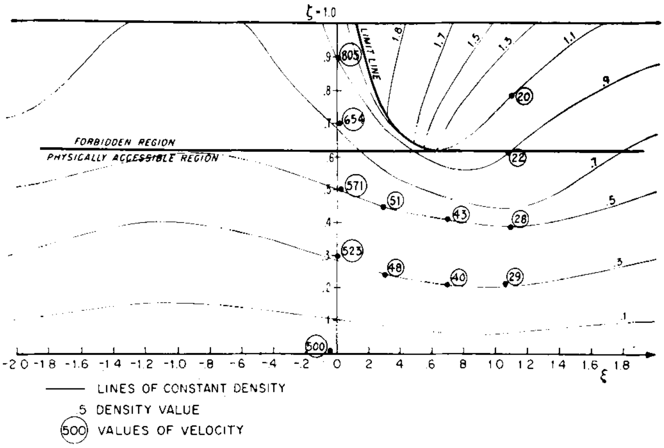

Fig. 11. Cross stream structure of a constant potential vorticity jet with uniform bottom temperature.

tary vorticity. (See BLANFORD [1965].) The continuous density model version of this breakdown is the intrusion of a limit-line into the solution region.

7. The equilibrium of free stream and open ocean

7.1. CHANGE OF TRANSPORT PHENOMENA

The divergent state equations (5.4b, 6b, 10b) may be combined to yield a single equation for Π_{01}, from which the other fields are simply deriveable. In this section the $_{01}$-subscript will be suppressed, and the definition $v_{00} \equiv V$ will be adopted. Thus

$$\Pi_{\xi\xi} + \Pi_{\theta\theta} = 0, \qquad (7.1)$$

with the conditions (5.11b) on θ_{00} (1), θ_{00} (0)

$$V_\theta \Pi - V\Pi_\theta + V[V_\theta \Pi_\xi - V_\xi \Pi_\theta] = 0. \qquad (7.2)$$

At the open ocean sides the divergence is forced by

$$\Pi^G = \mathcal{T}^{\pm}\theta - \mathcal{U}^{\pm}. \qquad (7.3)$$

Equation (7.3) exhibits the solution of (7.1) which is independent of ξ. Since the Π problem is homogeneous, (7.3) must be the limiting form of an eigenfunction as $|\xi| \to \infty$; $(\mathcal{U}/\mathcal{T})^{\pm}$ will be seen to play the roles of eigenparameters. In the limit as $\xi \to \pm\infty$ let $V \sim v$, θ_{00} (1) $\sim 1 + \mathcal{T}_{00} + \mathcal{V}_{00}$ (1), $\theta_{00}(0) \sim \mathcal{T}_{00} + \mathcal{V}_{00}(0)$ (with $\pm$ signs suppressed). The boundary conditions assume the limiting form

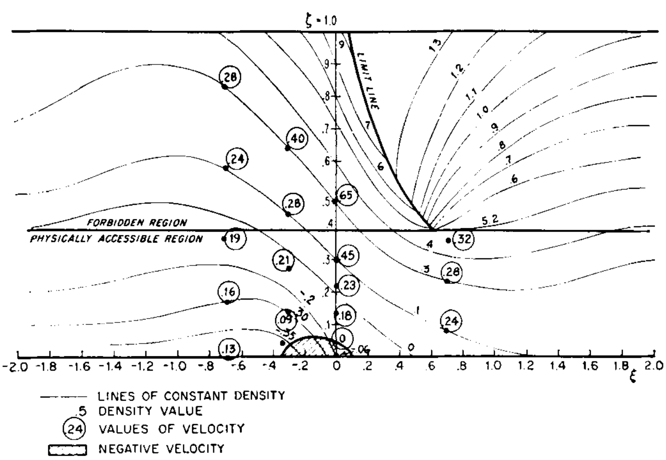

Fig. 12. Cross stream structure of a constant potential vorticity jet with variable bottom temperature.

$$\Pi^G - k_{1,0}\Pi_\theta^G = 0, \tag{7.4}$$

on $\theta_{00} = 1 + \mathcal{J}_{00}$, $\mathcal{J}_{00}$.
The notation in (7.4) is similar to that used in Section 4, i.e.

$$k_1 = (\nu/\nu_\theta)\,|_{\theta=1+\mathcal{J}_{00}}, \quad k_0 = (\nu/\nu_\theta\,|_{\theta=\mathcal{J}_{00}}. \tag{7.5}$$

It now follows from (7.3) and (7.4) that the eigenconditions for existence of a geostrophic flux at the seaward edges of the jet are

$$k_1 = 1 + k_0, \quad (\mathcal{U}/\mathcal{J}) = -k_0 + \mathcal{J}_{00}. \tag{7.6}$$

The first of (7.6) is a condition on the initial jet which allows a divergence on an f-plane of constant depth. The simply decaying jet of § 6 has asymptotically the velocity profile $\nu^{\pm} = V_0 \sin \alpha_0[\theta + \theta_1]\, e^{\pm \alpha_0 \xi}$. The eigencondition on the initial jet can now be written, for $\gamma = (\theta_1 + \mathcal{J}_0)\,\alpha_0$,

$$\tan(\alpha_0 + \gamma) = \alpha_0 + \tan \gamma. \tag{7.7}$$

A graphical analysis of (7.7) shows that this equation can be satisfied only for $\alpha_0 \geqslant \pi(\gamma = \pm\pi/2$ when the equality sign applies). This implies that such a jet can efflux mass (in this model) on an f-plane of constant depth only if the velocity profile changes sign with depth at its open ocean edges. The decrease in total mass is given by

$$Q = \varepsilon_\eta \left[\int_0^1 (u^{G+} - u^{G-})\,d\zeta\right] = \varepsilon\eta[\tfrac{1}{2}(\mathcal{J}^- - \mathcal{J}^+) + (k_0^- \mathcal{J}^- - k_0^+ \mathcal{J}^+)]. \tag{7.8}$$

A component of the net divergence is proportional to the difference of a forced thermal wind shear, characterized by $\mathcal{J}^{\pm}$, the downstream slope of isotherms. In addition, there is a contribution from the difference of a barotropic component of efflux, proportional to $(\mathcal{J}k_0)^{\pm}$. This contribution is associated with the difference of ζ-profiles on the right and left sides of the jet (a cross-stream ζ-profile *asymmetry*).

The existence of an efflux at $|\xi| \to \infty$ does not necessarily mean that the flux can be continued through the jet in a regular manner. This can, however, be demonstrated for small asymmetry of the initial jet and a small initial dynamic pressure difference across the jet (i.e. in Section 6, $\mathcal{J}$, $\mathcal{C} < 1$). For this case the

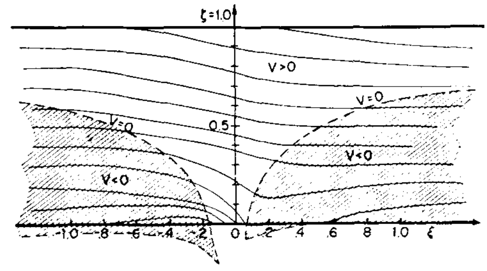

Fig. 13. Schematic cross-stream structure of a constant potential vorticity jet consistent with a uniform divergence.

boundary conditions (7.2) have the approximate form on $\theta = 1, 0$

$$\Pi = k_{1,0}\Pi_\theta, \tag{7.9}$$

where $k_{1,0} = (V/V_\theta)\,|_{\theta=1,0}$. The simplest form of small allowed asymmetry of the initial jet may be characterized by $k_1 = 1 + k(\xi)$, $k_0 = k(\xi)$, where $|k| < 1$, and $k \to O$ as $\xi \to +\infty$, $k \to k$ as $\xi \to -\infty$. The solution of the equations for an initial jet of constant potential vorticity (v_{00}) which satisfies the required boundary conditions has been obtained by similar methods as were used in Section 6. Here only a schematic diagram for the jet cross-sectional profile is presented. Fig. 13 is a picture of the initial jet for small monotonic $k > 0$. When $k = 0$, $v_{00}(0) = 0$, and the lines of velocity inversion form a cusp at $\xi = 0$.

To the order where asymmetry is neglected $\Pi = \mathcal{J}\theta$, and the flux of fluid which passes in one side of the weak symmetric jet must reappear at the other side. To order k, the solution is written as

$$\Pi = [\theta + k(1 - \tfrac{3}{2}\theta)] + \sum_1^\infty \varphi_n(\xi) \sin \lambda_n \theta, \tag{7.10}$$

where $$\tan \lambda_n = \lambda_n,\ \lambda_n \neq 0. \tag{7.11}$$

Here the ξ dependence is determined from the particular solutions of

$$\frac{d^2\varphi_n}{d\xi^2} - \lambda_n^2 \varphi_n = 4k'' \frac{\lambda_n(1 - \cos \lambda_n)}{(2\lambda_n - \sin 2\lambda_n)}. \tag{7.12}$$

As $|\xi| \to \infty$, $k'' \to 0$ and hence $\varphi_n \to 0$. The net loss of mass is the given by $\frac{1}{4}\,\varepsilon nk\mathcal{J}$.

It should be pointed out that in general the divergence phenomena for free jets (even for this model) is not completely understood. Only the simplest features of a free jet which can lead to a net divergence have been described here; a more complete investigation of this problem would itself present a fascinating study.

7.2. A MEANDER SCALE PHENOMENON

It is of interest to consider further the asymptotic analysis of the structural problem introduced in Section 4. There the radiated wave induced by the meandering was discussed for the case of constant potential vorticity by equations subsequently derived in Section 5 (formally for $\varepsilon = \beta^* = 0$). The additional meander induced structural feature for this case to be discussed here is a jet width change. A succinct exposition of this phenomenon is accomplished by rendering the δ-expansion uniformly valid in ξ.

An asymptotic decomposition of the pressure field is made as in Sections 4 and 7.1 viz., $\Pi_1 \sim \Pi^M + \pi_1$, $v_0 \sim \nu_0$, as $\xi \to \infty$. Whence,

$$\pi_{1\xi\xi} + \pi_{1\theta\theta} = -\varkappa_0 \nu_0. \tag{7.13}$$

On $\theta = 1 + \mathcal{T}_0$, $\mathcal{T}_0$

$$\nu_{0\theta}\pi_1 - \nu_0 \pi_{1\theta} = -\vartheta_0 \nu_{0\theta\theta} \Pi_1^M + \nu_{0\xi}\nu_0 \Pi_{1\theta}^M \tag{7.14}$$

$$\nu_{00}\pi_1 - \nu_0 \pi_{1\theta} = -\vartheta_0 \nu_{0\theta\theta} \Pi_1^M + \nu_{0\xi}\nu_0 (\Pi_{1\theta}^M + B). \tag{7.15}$$

(As usual ($\pm$) will be written explicitly only for emphasis). From (6.10) and (7.13) it can be seen that a particular solution for π_1 is proportional to $\xi \nu_0$. Hence, in the limit $\delta \to 0$ the ratio of v_1 to v_0 contains a term $0(\xi\delta)$. The formal expansion scheme used here implies that in the decaying portion of the jet terms of $0(\delta\xi)$ dominate those of $0(\delta)$, i.e. the edge of the jet is defined in the limit $\delta \to 0$ with $\delta\xi = o(1)$. Note that this small order symbol has the interpretation that for large ξ $0(\delta) < \delta\xi < 1$. This indicates that Π_0 is a non-uniform approximation in ξ to the full solution of equations in the limit of small δ. To remove this non-uniformity, a modified Poincaré-Lighthill method of expansion of the variables is adopted [e.g. vid. LIGHTHILL, (1949)]. It might be remarked that the effects of convergence of constant η lines also yields similar terms in the δ-expansion of the problem. This effect is of $0(\delta^2\xi)$ and represents a non-uniformity in the $\Pi_0 + \delta\Pi_1$ approximation to the full equations in the limit of small δ^2, and is of higher order than has been considered here.

In the limit of large ξ, let

$$\Pi \sim \Pi_0^G(\theta) + \pi_0(\xi,\theta)\Phi[\delta b(\eta)\xi] + \delta b(\eta) \times [\Pi_1^M(\theta) + \pi_1(\theta,\xi)] + 0(\delta^2\xi). \tag{7.16}$$

Consider the simple case of constant initial bottom temperature where $\mathcal{T}_0 = 0$, $\nu_{0\theta} = 0$, $k_0 \to \infty$. The radiated field is determined from Section 4 as

$$\Pi_1^M = -[k_1 + \theta - 1]. \tag{7.17}$$

Then the modified equation is

$$\pi_{1\xi\xi} + \pi_{1\theta\theta} = q\nu_0\Phi - 2\nu_0\Phi', \quad q = (\bar{v}_0/\langle v_0^2\rangle), \tag{7.18}$$

and on $\theta = 1$, 0, there obtains with the help of (6.8)–(6.10),

$$\pi_1 - k_1\pi_{1\theta} = \pm 2\alpha_0 k_1 \nu_0 \Phi, \tag{7.19}$$

$$\pi_{1\theta} = 0. \tag{7.20}$$

The inhomogeneity in the boundary condition (7.19) is removed by defining the function

$$\hat{\pi}_1 \equiv \pi_1 \mp 2\alpha_0 k_1 \nu_0(\xi, 1)\Phi. \tag{7.21}$$

It then follows that (7.18)–(7.20) become

$$\hat{\pi}_{1\xi\xi} + \hat{\pi}_{1\theta\theta} = \mp 2\alpha_0^3 k_1 \nu_0(\xi, 1)\,\Phi - \nu_0(\xi,\theta)[2\Phi' - q\Phi] \tag{7.22}$$

$$\hat{\pi}_1 - k_1\hat{\pi}_{1\theta} = 0 \tag{7.23}$$

$$\hat{\pi}_{1\theta} = 0. \tag{7.24}$$

The particular solution for $\hat{\pi}_1$ can be expanded in the series

$$\hat{\pi}_{1p} = \sum_0^\infty \varphi_n(\xi)\cos q_n\theta \pm \left[\Phi' - \frac{q}{2}\Phi\right]\frac{\xi}{\alpha_0}\nu_0, \tag{7.25}$$

where the eigenvalues are determined from

$$q_n \tan q_n = -(1/k_1). \tag{7.26}$$

The equation for $\varphi_n(\xi)$ follows from (7.22)

$$\varphi_{n\xi\xi} - q_n^2\varphi_n = \mp 4\alpha_0^3 k_1 \nu_0(\xi,1)\Phi \times \left[\frac{\sin q_n}{q_n(1+\sin 2q_n/2q_n)}\right]. \tag{7.27}$$

Since ν_0 is an eigenfunction of the $\hat{\pi}_1$ problem,

$q_0 = \alpha_0$ is secular. With this observation,

$$\hat{\pi}_{1p} = \mp \frac{\xi}{\alpha_0} \left\{ \left[\frac{q}{2} \pm \frac{2\alpha_0^2 \cos^2 \alpha_0}{(1+\sin 2\alpha_0/2\alpha_0)} \right] \Phi - \Phi' \right\} v_0 + \\ + \sum_1^\infty \pm \frac{4\alpha_0^3 k_1 v_0(\xi, 1) \cos q_n \theta}{q_n [q_n^2 - \alpha_0^2][1 + \sin 2q_n/2q_n]}. \quad (7.28)$$

The non-uniformity in ξ is now removed from the particular solution by chosing

$$\Phi = \exp \left\{ \left[\frac{q}{2} \pm \frac{4\alpha_0^3 \cos^2 \alpha_0}{(2\alpha_0 + \sin 2\alpha_0)} \right] \delta b(\eta) \xi \right\}. \quad (7.29)$$

The appearance of $b(\eta)$ in the argument of the exponential of (7.29) indicates that the lowest order effect of meandering is a change in width of the initial jet. The mass change (wave radiation) is slightly higher order. If $b(\eta) > 0$ the jet moves into shallow water and becomes broader. The jet moving into deep water narrows. To $0(\delta, \xi)$, the mass of the jet is conserved, and stretching of a finite, constant mass vortex sheet ($b < 0$) tends to increase its strength and make it narrower, while compressing a finite vortex sheet ($b > 0$) tends to decrease its strength and make it broader. Fig. 10 indicates in a schematic way the meandering induced effects of a constant potential vorticity and constant transport jet.

Acknowledgement

This work was supported in part by the National Science Foundation under a grant (No. GP-3533) for research in oceanic dynamics and in part by the Office of Naval Research under a contract (NONR 1866 (51)) to Harvard University.

REFERENCES

Blanford, R., 1965, Inertial flow in the Gulf Stream, *Tellus*, **17**, 1, pp. 69–76.

Crease, J., 1962, Velocity measurements in the deep water of the western North Atlantic, *J. Geophys. Res.*, **67**, pp. 3173–3176.

Goldstein, S., ed. 1938, Modern Developments in Fluid Mechanics, V. 1, p. 119, Oxford Press.

Fofonoff, N., 1965, Private communication.

Fuglister, F. C., & Worthington, L. V., 1951, Some results of a multiple ship survey of the Gulf Stream, *Tellus*, **3**, pp. 1–14.

Fuglister, F. C., 1963, Gulf Stream '60, in Progress in Oceanograpny, V. 1, pp. 265–273.

Fuglister, F. C., & Voorhis, A. D., 1966, A method of tracking the Gulf Stream.

Iselin, C., O'D., 1961, An interpretation of the deep current measurements, *Oceanus*, **7**, **3**, p. 9.

Lighthill, M. J., 1949, A technique for rendering approximate solutions to physical problems uniformly valid, *Proc. Roy. Soc.*, Ser. **7**, **40**, **311**, pp. 1170–1201.

Robinson, A. R., 1965, Three-dimensional model of inertial currents in a variable-density ocean, *J. Fluid Mech.*, **21**, pp. 211–223.

Warren, B. A., 1963, Topographical influences on the path of the Gulf Stream, *Tellus*, **15**, 2, pp. 167–183.

ТЕОРИЯ СВОБОДНЫХ ИНЕРЦИАЛЬНЫХ ТЕЧЕНИЙ

I. *Траекторил и струкпиура*

Развита теория для равновесных течений, сохраняющих потенциальный вихрь и представляющих собой поток с большой относительной завихренностью, наложенной на геострофический дрейф. Включены эффекты топографии дна, стратификации и изменения параметра Кориолиса. Сделано преобразование к системе координат, движущейся по линиям тока, и произведено разложение по многим переменным в соответствии со многими масштабами, входящими в схему описания течений. Численно изучается набор траекторий, которым может следовать течение над дном с равномерным наклоном. Получены профили скорости в некоторых поперечных сечениях течения, согласающиеся с полной расходимостью потока. Важным результатом является то, что бароклинная меандрирующая струя с необходимостью обменивается массой с окружающим океаном, т. е. после стоячих геострофических волн является особенностью равновесия. Получено также расширение и сужение течений.